Formation of dodecaphenylporphodimethene *via* facile protonation of saddle-distorted dodecaphenylporphyrin†

Takahiko Kojima,*[a] Kakeru Hanabusa,[a] Kei Ohkubo,[a] Motoo Shiro[b] and Shunichi Fukuzumi*[a]

Received (in Cambridge, UK) 15th September 2008, Accepted 7th October 2008
First published as an Advance Article on the web 5th November 2008
DOI: 10.1039/b816063e

A saddle-distorted dodecaphenylporphyrin undergoes protonation followed by two-electron reduction by $SnCl_2$ to give a roof-shaped dodecaphenylporphodimethene which exhibits reversible one-electron reduction and oxidation behaviour in benzonitrile to allow us to observe an ESR spectrum of π-cation radical in the course of electrochemical oxidation.

Porphyrins can undergo reduction to produce a variety of hydroporphyrins including chlorin whose magnesium complex is chlorophyll which is a component of light-harvesting antennas complexes in photosystems for photosynthesis.[1] In the course of formation of chlorin, porphodimethene, which is another two-electron-reduced species of porphyrin with hydrogenation at the 5 and 15 positions, is believed to be formed as an intermediate.[2] Porphodimethene derivatives have been synthesized by the reaction of high-valent metal complexes of porphyrins due to elevated reduction potentials of metal-bound porphyrin ligands.[3] Porphodimethenes have so far been characterized by crystallographic and spectroscopic methods,[4] however, their redox properties and radical species as redox products have yet to be explored.

We would like to report herein the synthesis and characterization of dodecaphenylporphodimethene (**1**) which is available from the reaction of dodecaphenylporphyrin (H_2DPP)[5] with $SnCl_2$ in pyridine. We also describe the redox behaviour of **1** in benzonitrile (PhCN) to demonstrate reversible one-electron reduction and oxidation to give the π-anion and π-cation radicals of **1** and the detection of the π-cation radical ($\mathbf{1}^{+\bullet}$) by ESR spectroscopy in PhCN.

The reaction of H_2DPP with $SnCl_2{\cdot}2H_2O$ was conducted in pyridine at reflux for 24 h under N_2. Purification by column chromatography on activated alumina eluted with CH_2Cl_2 and recrystallization of a crude product from CH_2Cl_2–CH_3CN allowed us to isolate **1** as red crystals in 21% yield.[6] The compound **1** is stable and the reaction of **1** with dichlorodicyanoquinone does not afford H_2DPP.

X-ray crystallography of **1** established its crystal structure unambiguously as depicted in Fig. 1.‡ The compound **1** exhibited a roof-like shape which was typical of those observed for previously reported porphodimethenes. At the 5 and 15 positions, hydrogenation occurred to allow the two *meso* carbons to possess a tetrahedral geometry. The two phenyl groups at the 5 and 15 positions point in the same direction to take a *cis* configuration as found in other porphodimethene derivatives reported so far.[7]

The bond lengths (Å) for the hydrogenated carbons (C5 and C15) were determined to be 1.508(6) and 1.515(6) for C5–C4 and C5–C6, respectively, and 1.499(6) and 1.500(6) for C15–C14 and C15–C16, respectively. The bond lengths are longer than those of other C–C bonds involving C1–C20 in the porphyrinoid core to indicate that both carbons are in the sp^3 configuration.

A dihedral angle of the roof between the two mean planes including two pyrroles with N2 and N3 and with N1 and N4 was estimated to be 48.1° (131.9°). As for the distortion of the half of the roof, the dihedral angles between the two pyrrole planes were estimated to be 12.8° for those including N1 and N4, and 11.5° for those including N2 and N3, respectively. Compared to the saddle distortion observed in H_2DPP, **1** exhibits much smaller distortion due to the flipping out of the two *meso*-phenyl groups from steric congestion upon hydrogenation at the *meso* positions (C5 and C15 in Fig. 1).

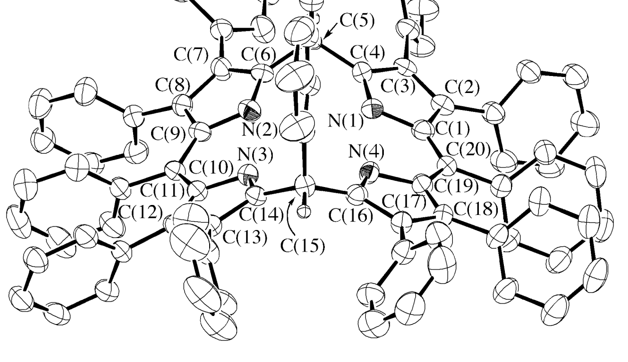

Fig. 1 An ORTEP drawing of **1**. Hydrogen atoms are omitted for clarity except the two *meso*-hydrogen atoms.

---

[a] *Department of Material and Life Science, Graduate School of Engineering, Osaka University and SORST (JST), 2-1 Yamada-oka, Suita, Osaka 565-0871, Japan. E-mail: kojima@chem.eng.osaka-u.ac.jp (T. K.). E-mail: fukuzumi@chem.eng.osaka-u.ac.jp (S. F.); Fax: +81 6-6879-7370; Tel: +81 6-6879-4734*

[b] *X-ray Research Laboratory, Rigaku Corporation, 3-9-12 Matsubara, Akishima-shi, Tokyo 196-8666, Japan*

† Electronic supplementary information (ESI) available: A CIF file of **1**, an ORTEP drawing of a partial structure of **1**, absorption spectrum (in CH_2Cl_2), an ORTEP drawing, and a CIF file of $[Sn(DPP)Cl_2]$, and the list of authors of ref. 9. CCDC 702272–702273. For ESI and crystallographic data in CIF or other electronic format see DOI: 10.1039/b816063e

In the absorption spectrum of **1** in CH_2Cl_2, a strong absorption was observed at 465 nm (ε = 6.96 × 10^4 dm^3 mol^{-1} cm^{-1}) and a weak shoulder band at 540 nm (ε = 6.14 × 10^3 dm^3 mol^{-1} cm^{-1}). H_2DPP has been reported to exhibit a Soret band at 468 nm and Q bands at 566, 618 and 712 nm in CH_2Cl_2.[8] Thus, the Q bands of **1** showed a blue shift because of the diminution of the extent of π-conjugation.

In the ^1H NMR spectrum of **1**, a singlet assigned to the methine protons at the hydrogenated *meso* positions was observed at 5.70 ppm in CD_2Cl_2 due to the deshielding by the π-current of the π-conjugation system. In addition, a singlet ascribed to the pyrrole N–H protons was found at 14.87 ppm, which was totally different from those observed for porphyrins in the negative chemical shift region. These observations clearly indicate that the electronic structure of **1** is different from that of H_2DPP.

A cyclic voltammogram (CV) of **1** in PhCN containing 0.1 mol dm^{-3} tetra-*n*-butylammonium hexafluorophosphate ($TBAPF_6$) as an electrolyte was measured and three reversible redox couples were observed at 1.00 (ΔE = 76 mV), –1.30 (ΔE = 74 mV) and –1.63 V (ΔE = 104 mV), relative to SCE, as shown in Fig. 2. Each redox couple was assigned to $\mathbf{1}^{0/+\bullet}$, $\mathbf{1}^{-\bullet/0}$, and $\mathbf{1}^{2-/-\bullet}$, respectively. The HOMO–LUMO gap for **1** is estimated to be 2.30 V based on the redox potentials of $\mathbf{1}^{0/+\bullet}$ and $\mathbf{1}^{-\bullet/0}$ redox couples and this value is consistent with the value calculated on the basis of the lowest absorption band (2.25 V). The reversibility in redox behaviour of **1** is in sharp contrast to that of H_2DPP: a CV of H_2DPP in CH_2Cl_2 shows only irreversible redox waves at 0.56 V as the anodic peak potential (E_{pa}) and at –1.28 V as the cathodic peak potential (E_{pc}).

Electrochemical oxidation of **1** in PhCN at room temperature at 0.94 V (*vs.* SCE) caused spectral change in absorption spectra as shown in Fig. 3(a) with two isosbestic points showing at 420 and 479 nm. Reverse electrochemical reduction at 0.19 V (*vs.* SCE) recovered the original spectrum of **1**. In the course of electrochemical oxidation of **1** at 1.04 V (*vs.* SCE) in PhCN at RT, we could observe an ESR spectrum ascribed to that of $\mathbf{1}^{+\bullet}$ at g = 2.0033 as shown in Fig. 3(b). The ESR spectrum of $\mathbf{1}^{+\bullet}$ exhibits no hyperfine splitting with the nitrogen nuclei, indicating a small population of unpaired electron density at the pyrrole nitrogen atoms in $\mathbf{1}^{+\bullet}$. On the other hand, electrochemical reduction at –1.36 V (*vs.* SCE) in PhCN gave irreversible spectral change in absorption spectra at room temperature.

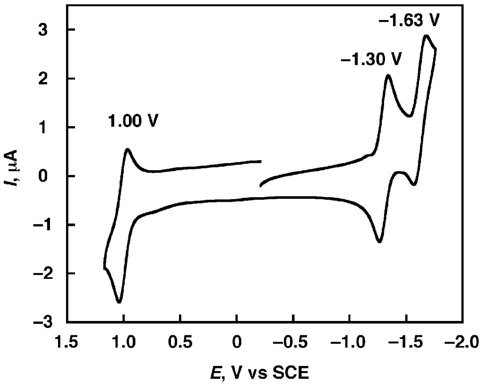

Fig. 2 Cyclic voltammogram of **1** in PhCN (0.1 mol dm^{-3} $TBAPF_6$) at room temperature under Ar: scan rate, 100 mV s^{-1}.

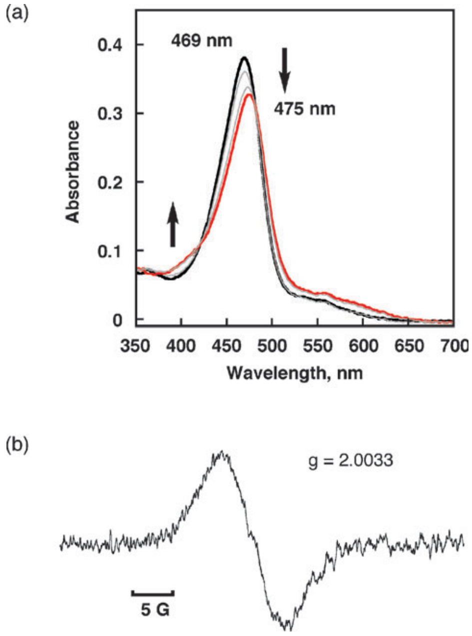

Fig. 3 (a) Absorption spectral change in the course of electrochemical oxidation of **1** at 0.94 V (*vs.* SCE) in PhCN (0.1 mol dm^{-3} $TBAPF_6$) at room temperature: black line for **1** and red line for the $\mathbf{1}^{+\bullet}$; (b) ESR spectrum of $\mathbf{1}^{+\bullet}$ in PhCN: Frequency, 9.362 GHz; modulation (100 kHz), 0.2 mT.

DFT calculations were performed on **1** and $\mathbf{1}^{+\bullet}$ to gain an understanding of their electronic structures.[9] The HOMO orbital of **1** is delocalized at the α and β positions of pyrroles and there is no contribution from orbitals of the pyrrole nitrogens and the *meso* sp^2-carbons as depicted in Fig. 4(a). The SOMO orbital of the one-electron-oxidized π-cation radical, $\mathbf{1}^{+\bullet}$, shows spin distribution mainly at the sp^2-*meso* carbons and pyrrole carbons and a small population (4%) at each pyrrole nitrogen as demonstrated in Fig. 4(b). Thus, calculated hyperfine coupling constants of the nitrogens are 0.0038 mT on average and this is too small to be detected. Due to the irreversibility of redox processes for H_2DPP, we could not make a comparison of ESR spectra of π-cation and π-anion radicals of **1** and those of H_2DPP.

We also gained a mechanistic insight into the formation of **1**. Upon addition of $SnCl_2{\cdot}2H_2O$ into the solution of H_2DPP in pyridine, we could observe the formation of

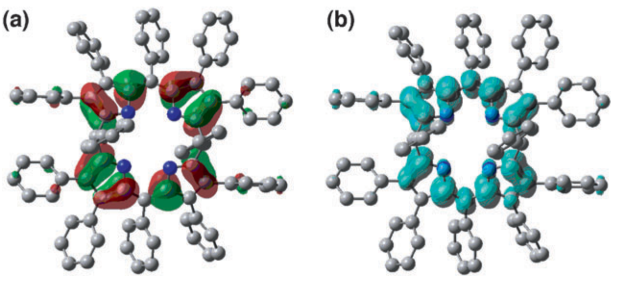

Fig. 4 (a) HOMO of **1** calculated at the B3LYP/6-31G(d) level of theory. (b) Spin distribution of $\mathbf{1}^{+\bullet}$ calculated at the UB3LYP/3-21G level of theory.

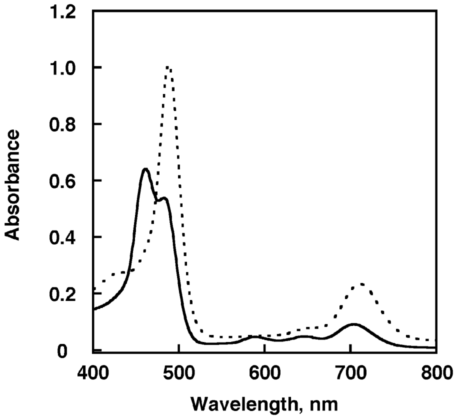

Fig. 5 Absorption spectra of the reaction mixture of H_2DPP and $SnCl_2{\cdot}2H_2O$ in pyridine: at the beginning of the reaction (dotted line) and at the end of the reaction (solid line).[10] Spectra were measured by adding an aliquot of the reaction mixture into CH_2Cl_2 as a solvent. Absorbance of each spectrum is not normalized.

H_4DPP^{2+} as represented by the absorption at 488 nm and 710 nm as shown in Fig. 5 (dotted line). This spectrum is consistent with that of $[H_4DPP]Cl_2$ in pyridine in the presence of an excess amount of HCl. Thus, we confirmed the formation of $[H_4DPP]Cl_2$ at the beginning of the reaction. This is due to the saddle-distortion of H_2DPP to facilitate protonation and to stabilize the diprotonated form as H_4DPP^{2+} with a larger saddle distortion.[8]

This protonation causes an anodic shift of the reduction potential of the porphyrin core to make H_4DPP^{2+} act as an electron acceptor.[8] In addition, the intermediacy of $[H_4DPP]Cl_2$ was assured by the formation of **1** by the reaction of $[H_4DPP]Cl_2$ and $SnCl_2{\cdot}2H_2O$ in pyridine under the same conditions.

$$SnCl_2 + H_2O \rightarrow SnCl(OH) + HCl \qquad (1)$$

$$H_2DPP + 2HCl \rightarrow H_4DPPCl_2 \qquad (2)$$

$$H_4DPPCl_2 + SnCl(OH) \rightarrow \mathbf{1} + SnCl_3(OH) \qquad (3)$$

$$SnCl_3(OH) + H_2O \rightarrow SnO_2 + 3HCl \qquad (4)$$

HCl can be generated from the reaction between $SnCl_2$ and water in pyridine, accompanied by the formation of SnCl(OH), in accordance with eqn (1).[11] SnCl(OH) has been reported to exhibit an oxidation potential of –0.47 V (*vs.* SCE),[12] which is appropriate for the reduction of H_4DPPCl_2 showing the two-electron reduction at –0.46 V (*vs.* SCE in CH_2Cl_2).[8] Insoluble white solid, which is assumed to be SnO_2, was formed at the end of the reaction. Thus, we propose that the reactions described in eqns (1)–(4) operate to give **1** as a product. The absorption spectrum of the reaction mixture exhibited two absorption maxima at 461 and 483 nm at the end of the reaction (Fig. 5, solid line). The final products contain **1** and $[Sn(DPP)Cl_2]$ as main products,[13] and unreacted $[H_4DPP]Cl_2$ that exhibits absorption denoted by a dotted line in Fig. 5.

In summary, we have developed a new strategy to synthesize a 5,15-dihydroporphodimethene derivative *via* the protonation of a metal-free porphyrin precursor to facilitate its reduction. We demonstrated reversible redox behaviour of **1** in electrochemical measurements for the first time. We could also observe reversible absorption spectral change in the course of electrochemical oxidation and the ESR spectrum of π-cation radical derived from the one-electron oxidation of **1**. Application of **1** to the formation of supramolecular assemblies and their photochemistry is underway in this laboratory.

Notes and references

‡ Crystal data for **1**: $C_{93}H_{66}Cl_2N_4$, monoclinic, $P2_1/n$, a = 15.042(3), b = 25.066(9), c = 19.584(4) Å, β = 111.594(5)°, V = 6866(3) Å^3, Z = 4, T = 123.1 K, μ(Mo Kα) = 1.48 cm^{-1}; No of reflections, 12 967; R_{int} = 0.086; $R1$ = 0.1097 ($I > 2\sigma(I)$), Rw = 0.2372 (all data), GOF = 1.122.

1 K. N. Ferreira, T. M. Iverson, K. Maghlaoui, J. Barber and S. Iwata, *Science*, 2004, **303**, 1831; P. Jordan, P. Fromme, H. T. Witt, O. Klukas, W. Saenger and N. Krauß, *Nature*, 2001, **411**, 909.

2 D. H. Burns, Y. H. Li, D. C. Shi and T. M. Caldwell, *J. Org. Chem.*, 2002, **67**, 4536; F.-P. Montforts, B. Gerlach and F. Höper, *Chem. Rev.*, 1994, **94**, 327.

3 K. M. Smith, in *The Porphyrin Handbook*, ed. K. M. Kadish, K. M. Smith and R. Guilard, Academic Press, San Diego, CA, 2000, vol. 1, p. 183.

4 M. Harmjanz and M. J. Scott, *Chem. Commun.*, 2000, 397; M. Harmjanz, I. Bozidarevic and M. J. Scott, *Org. Lett.*, 2001, **3**, 2281; M. Harmjanz, H. S. Gill and M. J. Scott, *J. Org. Chem.*, 2001, **66**, 5374; L. Bonomo, E. Solari, R. Scopelliti, C. Floriani and N. Re, *J. Am. Chem. Soc.*, 2000, **122**, 5312; X. Feng, I. Bischoff and M. O. Senge, *J. Org. Chem.*, 2001, **66**, 8693; M. O. Senge, S. Runge, M. Speck and K. Ruhlandt-Senge, *Tetrahedron*, 2000, **56**, 8927.

5 C. J. Medforth, M. O. Senge, K. M. Smith, L. D. Sparks and J. A. Shelnutt, *J. Am. Chem. Soc.*, 1992, **114**, 9859.

6 Elemental analysis for **1**; Calcd. for $C_{92}H_{64}N_4{\cdot}CH_2Cl_2{\cdot}3(H_2O)$: C, 81.86; H, 5.32; N, 4.11. Found: C, 81.59; H, 5.28; N, 3.95%. ^{1}H NMR δ_H (300 MHz; in CD_2Cl_2) 5.70 (2 H, s, *meso*-hydrogen), 6.24–7.43 (60 H, m, phenyl-H), 14.87 (2 H, N–H); m/z (MALDI-TOF-MS in CH_2Cl_2 (matrix: dithranol)) 1225.32 ([M – H]$^+$; $C_{92}H_{65}N_4$ requires 1225.52).

7 M. O. Senge, W. W. Kalisch and I. Bischoff, *Chem.–Eur. J.*, 2000, **6**, 2721; S. W. Rhee, Y. H. Na, Y. Do and J. Kim, *Inorg. Chim. Acta*, 2000, **309**, 49.

8 T. Kojima, T. Nakanishi, R. Harada, K. Ohkubo, S. Yamauchi and S. Fukuzumi, *Chem.–Eur. J.*, 2007, **13**, 8714; T. Kojima, T. Honda, K. Ohkubo, M. Shiro, T. Kusukawa, T. Fukuda, N. Kobayashi and S. Fukuzumi, *Angew. Chem., Int. Ed.*, 2008, **47**, 6712.

9 M. J. Frisch, *et al.*, *GAUSSIAN 03 (Revision C.02)*, Gaussian Inc., Wallingford, CT, 2004 (see Supplementary Information for the full list of authors).

10 In the absorption spectrum of $[Sn(DPP)(Cl)_2]$ in CH_2Cl_2, a Soret band was observed at 460 nm (ε = 2.97 × 10^5 dm^3 mol^{-1} cm^{-1}) and Q bands at 588 nm (ε = 1.85 × 10^4 dm^3 mol^{-1} cm^{-1}) and 645 nm (ε = 1.24 × 10^4 dm^3 mol^{-1} cm^{-1}). In addition, in the absorption spectrum of **1** a strong absorption was observed at 465 nm (ε = 6.96 × 10^4 dm^3 mol^{-1} cm^{-1}) and a weak shoulder band at 540 nm (ε = 6.14 × 10^3 dm^3 mol^{-1} cm^{-1}).

11 F. A. Cotton and G. Wilkinson, *Advanced Inorganic Chemistry*, John Wiley & Sons, New York, 1980, 4th edn, p. 397.

12 *CRC Handbook of Chemistry and Physics*, CRC Press, Boca Raton, 2001, 82nd edn, pp. 8–29; $SnO_2 + 3H^+ + 2e^- \rightleftharpoons SnOH^+ + H_2O$ (–0.194 V *vs.* NHE).

13 The formation of $[Sn(DPP)Cl_2]$ was confirmed by absorption and ^{1}H NMR spectroscopies, elemental analysis, and X-ray crystallography. A single crystal of the complex was obtained by recrystallization of the crude product from $CHCl_3$–hexane solution. See Supplementary Information. Crystal data for $[Sn(DPP)Cl_2]{\cdot}CHCl_3$: $C_{93}H_{61}Cl_5N_4Sn$, orthorhombic, *Pnma*, a = 11.7235(2), b = 28.4110(7), c = 21.1529(5) Å, V = 7045.5(3) Å^3, Z = 4, T = 123.1 K, μ(Mo Kα) = 0.606 cm^{-1}; No of reflections,6450; R_{int} = 0.067; $R1$ = 0.0827 ($I > 2\sigma(I)$), Rw = 0.2358 (all data), GOF = 1.036.